

# Analysis of two-spheres radiation problems by using the null-field integral equation approach

Ying-Te Lee<sup>1\*</sup> and Jeng-Tzong Chen<sup>1,2</sup>

<sup>1</sup>Department of Harbor and River Engineering

National Taiwan Ocean University, Keelung, Taiwan

<sup>2</sup>Department of Mechanical and Mechatronics Engineering

National Taiwan Ocean University, Keelung, Taiwan

\*D93520002@mail.ntou.edu.tw

NSC PROJECT: NSC 96-2221-E-019-041

## ABSTRACT

In this paper, a system approach, null-field integral equation in conjunction with the degenerate kernel, is used to solve the radiation problem of two spheres. The null-field integral equation instead of the conventional boundary integral equation can avoid the singular and hypersingular integrals. To fully utilize the spherical geometry, the fundamental solutions and the boundary densities are expanded by using degenerate kernels and spherical harmonics in the spherical coordinate, respectively. The main difference between the present approach and the conventional boundary integral equation is that the collocation point can be exactly located on the real boundary owing to introducing the degenerate kernel. The proposed approach is seen as one kind of semi-analytical methods, since the error is attributed from the truncation of spherical harmonics in the implementation. For the single sphere, the present approach can obtain the analytical solution. Finally, a two-spheres radiation problem is given to verify the validity of proposed approach.

**Keywords:** radiation, null-field integral equation, degenerate kernel, spherical harmonics, semi-analytical method

## 1. INTRODUCTION

It is well known that boundary integral equation methods (BIEMs) have been used to solve radiation and scattering problems for many years. The importance of the integral equation in the solution, both theoretical and practical, for certain types of boundary value problems is universally recognized. One of the problems frequently addressed in BIEM/BEM is the problem of irregular frequencies in boundary integral formulations for exterior acoustics and water wave problems. These frequencies do not represent any kind of physical resonance but are due to the numerical method, which has non-uniqueness solutions at characteristic frequencies associated with the eigenfrequency of the interior problem. Burton and Miller approach [1] as well as CHIEF technique [2] have

been employed to deal with these problems.

Regarding the irregular frequency, a large amount of papers on acoustics have been published. For example, numerical examples for non-uniform radiation and scattering problems by using the dual BEM were provided and the irregular frequencies were found [3]. The non-uniqueness solution of radiation and scattering problems are numerically manifested in a rank deficiency of the influence coefficient matrix in BEM [1]. In order to obtain the unique solution, several integral equation formulations that provide additional constraints to the original system of equations have been proposed. Burton and Miller [1] proposed an integral equation that was valid for all wave numbers by forming a linear combination of the singular integral equation and its normal derivative. However, the calculation for the hypersingular integration is required. To avoid the computation of hypersingularity, Schenck [2] used an alternative method, the CHIEF method, which employs the boundary integral equations by collocating the interior point as an auxiliary condition to make up deficient constraint condition. Many researchers [4-6] applied the CHIEF method to deal with the problem of fictitious frequencies. If the chosen point locates on the nodal line of the associated interior eigenproblem, then this method may fail. To overcome this difficulty, Seybert and Rengarajan [4] and Wu and Seybert [5] employed a CHIEF-block method using the weighted residual formulation for acoustic problems. On the contrary, only a few papers on water wave can be found. For water wave problems, Ohmatsu [7] presented a combined integral equation method (CIEM), which was similar to the CHIEF-block method for acoustics proposed by Wu and Seybert [5]. In the CIEM, two additional constraints for one interior point result in an overdetermined system to insure the removal of irregular frequencies. An enhanced CHIEF method was also proposed by Lee and Wu [6]. The main concern of the CHIEF method is how many numbers of interior points are required and where the positions should be located.

Recently, the appearance of irregular frequency in the method of fundamental solutions was theoretically

proved and numerically implemented [8]. However, as far as the present authors are aware, only a few papers have been published to date reporting on the efficacy of these methods in radiation and scattering problems involving more than one vibrating body. For example, Dokumaci and Sarigül [9] discussed the fictitious frequency of radiation problem of two spheres. They used the surface Helmholtz integral equation (SHIE) and the CHIEF method to examine the position of fictitious frequency. In our formulation, we are also concerned with the fictitious frequency especially for the multiple spheres of scatters and radiators. We may wonder if there is one approach free of both Burton and Miller approach and CHIEF technique to deal with irregular frequencies.

In the recent years, Chen and his group used the null-field integral equation formulation in conjunction with degenerate kernel and Fourier series to deal with many engineering problem with circular boundaries, such as torsion bar [10], water wave [11], Stokes flow [12], plate vibrations [13] and piezoelectricity problems [14]. They claimed that the approach has high accuracy and is one kind of semi-analytical approach. However, their applications only focused on problems of two-dimensional domain. In this paper, we would like to extend this idea to three-dimensional problems.

In this paper, a system approach, the null-field integral equation method in conjunction with the degenerate kernel, is used to study on the radiation problems of one and two spheres. By using the null-field integral equation instead of the boundary integral equation, we can avoid the singular and hypersingular integrals. To fully utilize the spherical geometry, the fundamental solutions and the boundary densities are expanded by using degenerate kernels and spherical harmonics, respectively. In this approach, the collocation point can be exactly located on the real boundary after introducing the degenerate kernel. The proposed approach is seen as one kind of semi-analytical methods, since the error only stems from the truncation of spherical harmonics. For the radiation of one sphere, the analytical solution can be derived via the proposed approach. Besides, a two-spheres radiation example is given to verify the validity of proposed approach.

## 2. PROBLEM STATEMENT AND THE PRESENT APPROACH

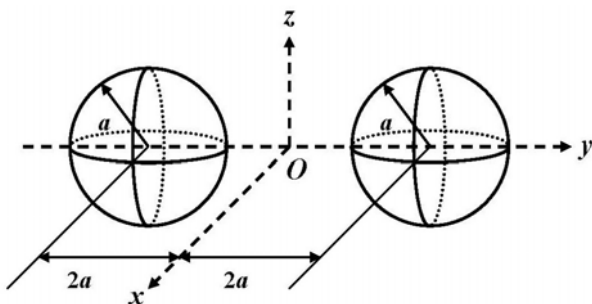


Fig. 1 Sketch of two spheres

### 2.1 Problem statement

The problem considered here is the radiation problem vibrating by two spheres. This problem is governed by the Helmholtz equation as follows:

$$(\nabla^2 + k^2)u(x) = 0, \quad x \in D, \quad (1)$$

where  $u(x)$  is the velocity potential,  $\nabla^2$  is the Laplacian operator,  $k$  and  $D$  denote the wave number and the domain of interest, respectively. Two spheres are shown in Fig. 1. The radius of two identical spheres is  $a$ .

### 2.2 Dual boundary integral equation formulation — the conventional version

The dual boundary integral formulation for the domain point is shown below:

$$u(x) = \int_S T(s, x)u(s)dS(s) - \int_S U(s, x)t(s)dS(s), \quad x \in D, \quad (2)$$

$$t(x) = \int_S M(s, x)u(s)dS(s) - \int_S L(s, x)t(s)dS(s), \quad x \in D, \quad (3)$$

where  $x$  and  $s$  are the field and source points, respectively, “ $S$ ” is the spherical surface,  $t(s)$  is the normal derivative on the source point, and the kernel function  $U(s, x)$  is the fundamental solution which satisfies

$$(\nabla^2 + k^2)U(s, x) = \delta(x - s), \quad (4)$$

where  $\delta$  is the Dirac-delta function. The other kernel functions can be obtained as

$$T(s, x) = \frac{\partial U(s, x)}{\partial n_s}, \quad (5)$$

$$L(s, x) = \frac{\partial U(s, x)}{\partial n_x}, \quad (6)$$

$$M(s, x) = \frac{\partial^2 U(s, x)}{\partial n_x \partial n_s}, \quad (7)$$

where  $n_x$  and  $n_s$  denote the outward normal vector at the field point and the source point, respectively. If the collocation point  $x$  is on the boundary, the dual boundary integral equations for the boundary point can be obtained as follows:

$$\frac{1}{2}u(x) = C.P.V. \int_S T(s, x)u(s)dS(s) - R.P.V. \int_S U(s, x)t(s)dS(s), \quad x \in B, \quad (8)$$

$$\frac{1}{2}t(x) = H.P.V. \int_S M(s, x)u(s)dS(s) - C.P.V. \int_S L(s, x)t(s)dS(s), \quad x \in B, \quad (9)$$

where  $R.P.V.$ ,  $C.P.V.$  and  $H.P.V.$  are the Riemann principal value, the Cauchy principal value and the Hadamard (or called Mangler) principal value, respectively. By collocating  $x$  outside the domain, we obtain the null-field integral equation as shown below:

$$0 = \int_S T(s, x)u(s)dS(s) - \int_S U(s, x)t(s)dS(s), \quad x \in D^c, \quad (10)$$

$$0 = \int_S M(s, x)u(s)dS(s) - \int_S L(s, x)t(s)dS(s), \quad x \in D^c, \quad (11)$$

where  $D^c$  denotes the complementary domain.

### 2.3 Dual null-field integral equation formulation — the present version

By introducing the degenerate kernels, the collocation points can be located on the real boundary free of facing singularity. Therefore, the representations of integral equations including the boundary point can be written as

$$u(x) = \int_S T^e(s, x)u(s)dS(s) - \int_S U^e(s, x)t(s)dS(s), \quad x \in D \cup S, \quad (12)$$

$$t(x) = \int_S M^e(s, x)u(s)dS(s) - \int_S L^e(s, x)t(s)dS(s), \quad x \in D \cup S, \quad (13)$$

and

$$0 = \int_S T^i(s, x)u(s)dS(s) - \int_S U^i(s, x)t(s)dS(s), \quad x \in D^c \cup S, \quad (14)$$

$$0 = \int_S M(s, x)u(s)dS(s) - \int_S L(s, x)t(s)dS(s), \quad x \in D^c \cup S, \quad (15)$$

once the interior “ $i$ ” or exterior “ $e$ ” kernel is expressed in terms of an appropriate degenerate form. It is found that the collocation point is categorized to three positions, domain (Eqs.(2)-(3)), boundary (Eqs.(8)-(9)) and complementary domain (Eqs.(10)-(11)) in the conventional formulation. After using the degenerate kernel for the null-field BIEM, both Eqs.(12)-(13) and Eqs.(14)-(15) can contain the boundary point.

### 2.4 Expansions of the fundamental solution and boundary density

The fundamental solution as previously mentioned is

$$U(s, x) = \frac{e^{-ikr}}{4\pi r}, \quad (16)$$

where  $r \equiv |s - x|$  is the distance between the source point and the field point and  $i$  is the imaginary number with  $i^2 = -1$ . To fully utilize the property of spherical geometry, the mathematical tools, degenerate (separable or of finite rank) kernel and spherical harmonics, are utilized for the analytical calculation of boundary integrals.

#### 2.4.1 Degenerate (separable) kernel for fundamental solutions

In the spherical coordinate, the field point,  $x$ , and source point,  $s$ , can be expressed as  $x = (\rho, \phi, \theta)$  and  $s = (\bar{\rho}, \bar{\phi}, \bar{\theta})$  in the spherical coordinate, respectively. By employing the addition theorem for separating the source point and field point, the kernel functions,  $U(s, x)$ ,  $T(s, x)$ ,  $L(s, x)$  and  $M(s, x)$ , are expanded in terms of degenerate kernel as shown below:

$$U(s, x) = \begin{cases} U^i = -\frac{ik}{4\pi} \sum_{n=0}^{\infty} (2n+1) \sum_{m=0}^n \varepsilon_m \frac{(n-m)!}{(n+m)!} \cos[m(\bar{\phi} - \phi)] \\ \quad P_n^m(\cos \bar{\theta}) P_n^m(\cos \theta) j_n(k\rho) h_n^{(2)}(k\bar{\rho}), \bar{\rho} \geq \rho, \\ U^e = -\frac{ik}{4\pi} \sum_{n=0}^{\infty} (2n+1) \sum_{m=0}^n \varepsilon_m \frac{(n-m)!}{(n+m)!} \cos[m(\bar{\phi} - \phi)] \\ \quad P_n^m(\cos \bar{\theta}) P_n^m(\cos \theta) j_n(k\bar{\rho}) h_n^{(2)}(k\rho), \bar{\rho} < \rho, \end{cases} \quad (17)$$

$$T(s, x) = \begin{cases} T^i = -\frac{ik^2}{4\pi} \sum_{n=0}^{\infty} (2n+1) \sum_{m=0}^n \varepsilon_m \frac{(n-m)!}{(n+m)!} \cos[m(\bar{\phi} - \phi)] \\ \quad P_n^m(\cos \bar{\theta}) P_n^m(\cos \theta) j_n(k\rho) h_n^{(2)}(k\bar{\rho}), \bar{\rho} > \rho, \\ T^e = -\frac{ik^2}{4\pi} \sum_{n=0}^{\infty} (2n+1) \sum_{m=0}^n \varepsilon_m \frac{(n-m)!}{(n+m)!} \cos[m(\bar{\phi} - \phi)] \\ \quad P_n^m(\cos \bar{\theta}) P_n^m(\cos \theta) j_n'(k\bar{\rho}) h_n^{(2)}(k\rho), \bar{\rho} < \rho, \end{cases} \quad (18)$$

$$L(s, x) = \begin{cases} L^i = -\frac{ik^2}{4\pi} \sum_{n=0}^{\infty} (2n+1) \sum_{m=0}^n \varepsilon_m \frac{(n-m)!}{(n+m)!} \cos[m(\bar{\phi} - \phi)] \\ \quad P_n^m(\cos \bar{\theta}) P_n^m(\cos \theta) j_n'(k\rho) h_n^{(2)}(k\bar{\rho}), \bar{\rho} > \rho, \\ L^e = -\frac{ik^2}{4\pi} \sum_{n=0}^{\infty} (2n+1) \sum_{m=0}^n \varepsilon_m \frac{(n-m)!}{(n+m)!} \cos[m(\bar{\phi} - \phi)] \\ \quad P_n^m(\cos \bar{\theta}) P_n^m(\cos \theta) j_n(k\bar{\rho}) h_n^{(2)}(k\rho), \bar{\rho} < \rho, \end{cases} \quad (19)$$

$$M(s, x) = \begin{cases} M^i = -\frac{ik^3}{4\pi} \sum_{n=0}^{\infty} (2n+1) \sum_{m=0}^n \varepsilon_m \frac{(n-m)!}{(n+m)!} \cos[m(\bar{\phi} - \phi)] \\ \quad P_n^m(\cos \bar{\theta}) P_n^m(\cos \theta) j_n'(k\rho) h_n^{(2)}(k\bar{\rho}), \bar{\rho} \geq \rho, \\ M^e = -\frac{ik^3}{4\pi} \sum_{n=0}^{\infty} (2n+1) \sum_{m=0}^n \varepsilon_m \frac{(n-m)!}{(n+m)!} \cos[m(\bar{\phi} - \phi)] \\ \quad P_n^m(\cos \bar{\theta}) P_n^m(\cos \theta) j_n'(k\bar{\rho}) h_n^{(2)}(k\rho), \bar{\rho} < \rho, \end{cases} \quad (20)$$

where the superscripts “ $i$ ” and “ $e$ ” denote the interior and exterior regions,  $j_n$  and  $h_n^{(2)}$  are the  $n^{\text{th}}$  order spherical Bessel function of the first kind and the  $n^{\text{th}}$  order spherical Hankel function of the second kind, respectively,  $P_n^m$  is the associated Legendre polynomial and  $\varepsilon_m$  is the Neumann factor,

$$\varepsilon_m = \begin{cases} 1, & m = 0, \\ 2, & m = 1, 2, \dots, \infty. \end{cases} \quad (21)$$

It is noted that  $U$  and  $M$  kernels in Eqs.(17) and (20) contain the equal sign of  $\rho = \bar{\rho}$  while  $T$  and  $L$  kernels do not include the equal sign due to discontinuity.

#### 2.4.2 Spherical harmonics expansion for boundary densities

We apply the spherical harmonics expansion to approximate the boundary density and its normal derivative on the surface of sphere. Therefore, the following expressions can be obtained

$$u_1(s) = \sum_{v=0}^{\infty} \sum_{w=0}^v A_{vw}^1 P_v^w(\cos \bar{\theta}) \cos(w\bar{\phi}), \quad s \in B_1, \quad (22)$$

$$u_2(s) = \sum_{v=0}^{\infty} \sum_{w=0}^v A_{vw}^2 P_v^w(\cos \bar{\theta}) \cos(w\bar{\phi}), \quad s \in B_2, \quad (23)$$

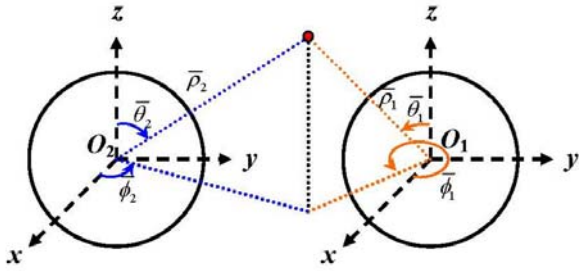


Fig. 2 Adaptive observer system

$$t_1(s) = \sum_{v=0}^{\infty} \sum_{w=0}^v B_{vw}^1 P_v^w(\cos \bar{\theta}) \cos(w \bar{\phi}), s \in B_1, \quad (24)$$

$$t_2(s) = \sum_{v=0}^{\infty} \sum_{w=0}^v B_{vw}^2 P_v^w(\cos \bar{\theta}) \cos(w \bar{\phi}), s \in B_2, \quad (25)$$

where  $A_{vw}^i$  and  $B_{vw}^i$  are the unknown spherical coefficients on  $B_i$  ( $i=1,2$ ). However, only  $M$  number of truncated terms for  $v$  is used in the real implementation.

### 2.5 Adaptive observer system

Since the boundary integral equations are frame indifferent, *i.e.* rule of objectivity is obeyed. Adaptive observer system is chosen to fully employ the property of degenerate kernels. Fig. 2 shows the boundary integration for the spherical boundaries. It is worthy of noting that the origin of the observer system can be adaptively located on the center of the corresponding circle under integration to fully utilize the geometry of sphere. The dummy variable in the integration on the surface are the angles ( $\bar{\theta}$  and  $\bar{\phi}$ ). By using the adaptive observer system, all the boundary integrals can be determined analytically without using the concept of principal value.

### 2.6 Linear Algebraic Equation

In order to calculate the  $P$  ( $P = (M + 2)(M + 1)/2$ ) unknown spherical harmonics,  $P$  boundary points on each spherical surface are needed to be collocated. By collocating the null-field point exactly on the  $k^{\text{th}}$  spherical surface for Eqs.(14) and (15) as shown in Fig. 2, we have

$$0 = \sum_{j=1}^N \int_{S_j} T^i(\mathbf{s}, \mathbf{x}_k) u(\mathbf{s}) dS(\mathbf{s}) - \sum_{j=1}^N \int_{S_j} U^i(\mathbf{s}, \mathbf{x}_k) t(\mathbf{s}) dS(\mathbf{s}), \quad \mathbf{x}_k \in D^c \cup S, \quad (26)$$

$$0 = \sum_{j=1}^N \int_{S_j} M^i(\mathbf{s}, \mathbf{x}_k) u(\mathbf{s}) dS(\mathbf{s}) - \sum_{j=1}^N \int_{S_j} L^i(\mathbf{s}, \mathbf{x}_k) t(\mathbf{s}) dS(\mathbf{s}), \quad \mathbf{x}_k \in D^c \cup S, \quad (27)$$

where  $N$  is the number of spheres. For the  $S_j$  boundary integral of the spherical surface, the kernels of  $U(\mathbf{s}, \mathbf{x})$ ,  $T(\mathbf{s}, \mathbf{x})$ ,  $L(\mathbf{s}, \mathbf{x})$  and  $M(\mathbf{s}, \mathbf{x})$  are respectively expressed in terms of degenerate kernels of Eqs. (17)-(20) with respect to the observer origin at the center of  $S_j$ . The

boundary densities of  $u(\mathbf{s})$  and  $t(\mathbf{s})$  are substituted by using the spherical boundary harmonics of Eqs. (22)-(25), respectively. In the  $S_j$  integration, we set the origin of the observer system to collocate at the center  $O_j$  of  $S_j$  to fully utilize the degenerate kernel and spherical harmonics. By locating the null-field point on the real surface  $S_k$  from outside of the domain  $D^c$  in the numerical implementation, linear algebraic systems are obtained as

$$[\mathbf{U}]\{\mathbf{t}\} = [\mathbf{T}]\{\mathbf{u}\}, \quad (28)$$

$$[\mathbf{L}]\{\mathbf{t}\} = [\mathbf{M}]\{\mathbf{u}\}, \quad (29)$$

where  $[\mathbf{U}]$ ,  $[\mathbf{T}]$ ,  $[\mathbf{L}]$  and  $[\mathbf{M}]$  are the influence matrices with a dimension of  $(N \times P)$  by  $(N \times P)$ , and  $\{\mathbf{t}\}$  and  $\{\mathbf{u}\}$  denote the vectors for  $t(\mathbf{s})$  and  $u(\mathbf{s})$  of the spherical harmonics coefficients with a dimension of  $(N \times P)$  by 1, in which,  $[\mathbf{U}]$ ,  $[\mathbf{T}]$ ,  $[\mathbf{L}]$ ,  $[\mathbf{M}]$ ,  $\{\mathbf{u}\}$  and  $\{\mathbf{t}\}$  can be defined as follows:

$$[\mathbf{U}] = [\mathbf{U}_{\alpha\beta}] = \begin{bmatrix} \mathbf{U}_{11} & \mathbf{U}_{12} & \cdots & \mathbf{U}_{1N} \\ \mathbf{U}_{21} & \mathbf{U}_{22} & \cdots & \mathbf{U}_{2N} \\ \vdots & \vdots & \ddots & \vdots \\ \mathbf{U}_{N1} & \mathbf{U}_{N2} & \cdots & \mathbf{U}_{NN} \end{bmatrix}, \quad (30)$$

$$[\mathbf{T}] = [\mathbf{T}_{\alpha\beta}] = \begin{bmatrix} \mathbf{T}_{11} & \mathbf{T}_{12} & \cdots & \mathbf{T}_{1N} \\ \mathbf{T}_{21} & \mathbf{T}_{22} & \cdots & \mathbf{T}_{2N} \\ \vdots & \vdots & \ddots & \vdots \\ \mathbf{T}_{N1} & \mathbf{T}_{N2} & \cdots & \mathbf{T}_{NN} \end{bmatrix}, \quad (31)$$

$$[\mathbf{L}] = [\mathbf{L}_{\alpha\beta}] = \begin{bmatrix} \mathbf{L}_{11} & \mathbf{L}_{12} & \cdots & \mathbf{L}_{1N} \\ \mathbf{L}_{21} & \mathbf{L}_{22} & \cdots & \mathbf{L}_{2N} \\ \vdots & \vdots & \ddots & \vdots \\ \mathbf{L}_{N1} & \mathbf{L}_{N2} & \cdots & \mathbf{L}_{NN} \end{bmatrix}, \quad (32)$$

$$[\mathbf{M}] = [\mathbf{M}_{\alpha\beta}] = \begin{bmatrix} \mathbf{M}_{11} & \mathbf{M}_{12} & \cdots & \mathbf{M}_{1N} \\ \mathbf{M}_{21} & \mathbf{M}_{22} & \cdots & \mathbf{M}_{2N} \\ \vdots & \vdots & \ddots & \vdots \\ \mathbf{M}_{N1} & \mathbf{M}_{N2} & \cdots & \mathbf{M}_{NN} \end{bmatrix}, \quad (33)$$

$$\{\mathbf{u}\} = \begin{Bmatrix} \mathbf{u}_1 \\ \mathbf{u}_2 \\ \vdots \\ \mathbf{u}_N \end{Bmatrix}, \quad \{\mathbf{t}\} = \begin{Bmatrix} \mathbf{t}_1 \\ \mathbf{t}_2 \\ \vdots \\ \mathbf{t}_N \end{Bmatrix}, \quad (34)$$

where the vectors  $\{\mathbf{u}_k\}$  and  $\{\mathbf{t}_k\}$  are in the form of  $\{A_{00}^k A_{10}^k A_{11}^k \cdots A_{pp}^k\}^T$  and  $\{B_{00}^k B_{10}^k B_{11}^k \cdots B_{pp}^k\}^T$ ; the first subscript “ $\alpha$ ” ( $\alpha = 1, 2, \dots, N$ ) in the  $[\mathbf{U}_{\alpha\beta}]$  denotes the index of the  $\alpha^{\text{th}}$  sphere where the collocation point is located and the second subscript “ $\beta$ ” ( $\beta = 1, 2, \dots, N$ ) denotes the index of the  $\beta^{\text{th}}$  sphere where the boundary data  $\{\mathbf{u}_k\}$  or  $\{\mathbf{t}_k\}$  are specified. The coefficient matrix of the linear algebraic system is partitioned into blocks, and each diagonal block ( $\mathbf{U}_{pp}$ ) corresponds to the influence matrices due to the same sphere of collocation and spherical harmonics expansion.

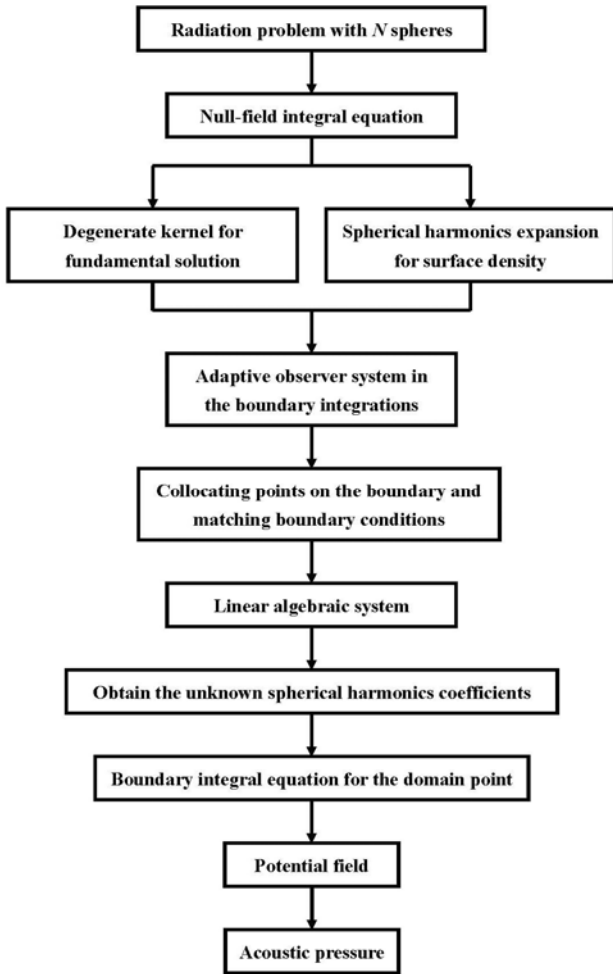


Fig. 3 The flowchart of the present method

After uniformly collocating the point along the  $\alpha^{th}$  spherical surface, the elements of  $[U_{\alpha\beta}]$ ,  $[T_{\alpha\beta}]$ ,  $[L_{\alpha\beta}]$  and  $[M_{\alpha\beta}]$  are defined as

$$U_{\alpha\beta} = \iint U(s_k, x_m) \bar{\rho}^2 d\bar{\phi}_k d\bar{\theta}_k, \quad (35)$$

$$T_{\alpha\beta} = \iint T(s_k, x_m) \bar{\rho}^2 d\bar{\phi}_k d\bar{\theta}_k, \quad (36)$$

$$L_{\alpha\beta} = \iint L(s_k, x_m) \bar{\rho}^2 d\bar{\phi}_k d\bar{\theta}_k, \quad (37)$$

$$M_{\alpha\beta} = \iint M(s_k, x_m) \bar{\rho}^2 d\bar{\phi}_k d\bar{\theta}_k, \quad (38)$$

where  $\bar{\phi}_k$  and  $\bar{\theta}_k$  ( $k = 1, 2, \dots, N$ ) are the spherical angles of the spherical coordinate for the source points. After obtaining the unknown spherical harmonics, interior potential can be obtained by employing Eq.(12). The flowchart of the present method is shown in Fig. 3.

### 3. NUMERICAL EXAMPLES

Here, three cases are given to demonstrate the validity of proposed approach. Cases 1 and 2 are one-sphere radiation problems subject to various boundary conditions. They can be seen as special cases. Case 3 is a two-spheres radiation problem with uniform radial velocity.

#### Case 1. A sphere pulsating with uniform radial velocity

In first case, one sphere is pulsating with uniform radial velocity  $U_0$ . The exact solution found in [15] is shown below:

$$p(\rho) = \frac{a}{\rho} \frac{iz_0 ka}{1 + ika} U_0 e^{-ik(\rho-a)}, \quad (39)$$

where  $z_0$  is the characteristic impedance of the medium  $z_0 = \rho_0 c$  in which  $\rho_0$  is the density of the medium at rest and  $c$  is the sound velocity, and  $p$  is the sound pressure which is defined as

$$p(\rho) = -i\rho_0 \omega u(\rho) = -iz_0 k u(\rho), \quad (40)$$

in which  $\omega$  is the angular frequency and  $k$  is the wave number that equals to the angular frequency over sound velocity. After expanding the surface density by using spherical harmonics, we have

$$B_{00} = U_0, \quad (41)$$

and the other coefficients are zero. Then, the unknown coefficient can be obtained as follows:

$$A_{00} = -\frac{1}{k} \frac{h_0^{(2)}(ka)}{h_0^{\prime(2)}(ka)} U_0, \quad (42)$$

by using Eq. (14). After obtaining the unknown coefficient, we have

$$p(\rho) = -iz_0 U_0 \frac{h_0^{(2)}(k\rho)}{h_0^{\prime(2)}(ka)}. \quad (43)$$

The present expression seems to vary from the exact solution in Eq. (39). However, the spherical Hankel function can be represented by using the series form found in [16] as shown below:

$$h_n^{(2)} = i^{n+1} z^{-1} e^{-iz} \sum_{m=0}^n \frac{(n+m)!}{m! \Gamma(n-m+1)} (-2iz)^{-m}. \quad (44)$$

After substituting Eq. (44) into Eq. (43), the result of our approach can yield the same exact solution of Eq. (39). Figs. 4(a) and 4(b) show the real and imaginary parts of non-dimensional pressure on the surface by using the numerical procedure which  $M$  is truncated in the finite number of terms. Here,  $M$  is chosen to be six and twenty nodes are distributed on the spherical surface as shown in Fig.4. In Figs. 5(a) and 5(b), irregular frequency does not appear due to the cancellation of zero divided by zero in our formulation. However, Seybert *et al.* [15] needed to improve their result by using the CHIEF method. For this

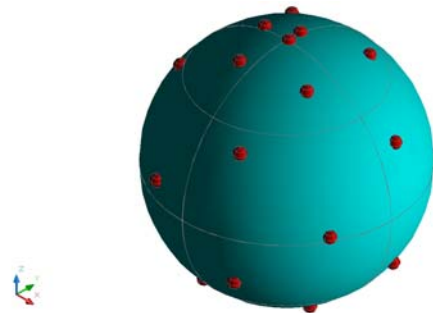
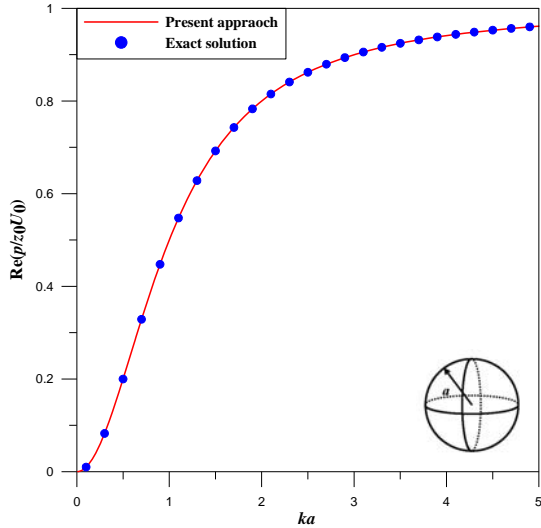
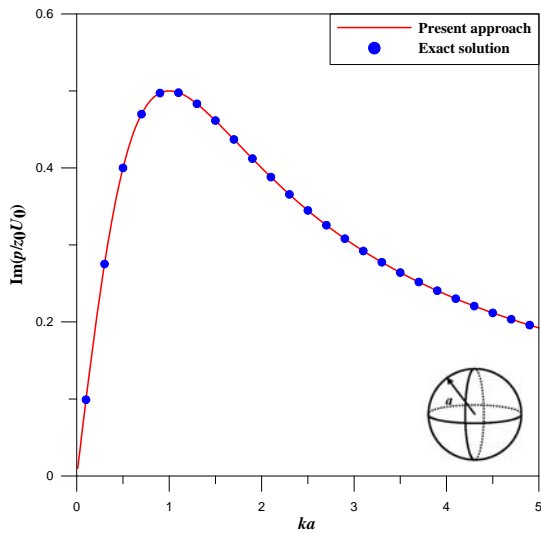


Fig. 4 Distribution of collocation points for a sphere



**Fig. 5(a) Real part of non-dimensional pressure on the surface**



**Fig. 5(b) Imaginary part of non-dimensional pressure on the surface**

point, we can claim that our approach is more accurate than that of Seybert *et al* [15].

**Case 2. A sphere oscillating with non-uniform radial velocity**

In this case, one sphere is oscillating with radial velocity  $U_0 \cos \theta$ . The exact solution is also found in [15] as

$$p(\rho, \theta) = \left(\frac{a}{\rho}\right)^2 \frac{iz_0 ka(1+ik\rho)}{2(1+ika) - k^2 a^2} (U_0 \cos \theta) e^{-ik(\rho-a)}. \quad (45)$$

After expanding the boundary density by using the spherical harmonics, we have

$$B_{10} = U_0, \quad (46)$$

and the other coefficients are zero. Then, the unknown coefficient can be obtained as follows:

$$A_{10} = -\frac{1}{k} \frac{h_1^{(2)}(ka)}{h_1^{\prime(2)}(ka)} U_0, \quad (47)$$

by using Eq. (14). After obtaining the unknown

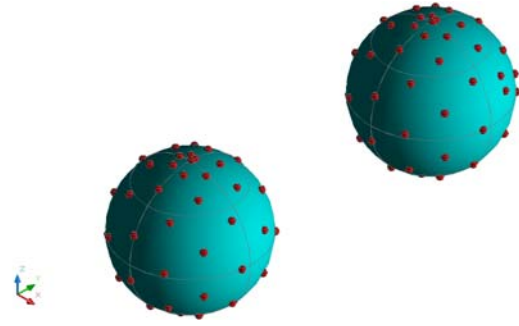


**Fig. 6 Distribution of collocation points for a sphere**

coefficient, we have

$$p(\rho, \theta) = -iz_0 U_0 \frac{h_1^{(2)}(k\rho)}{h_1^{\prime(2)}(ka)} \cos \theta. \quad (48)$$

Similarly, the present representation seems not to be equivalent to the exact solution of Eq.(45) for the first look. After substituting series form of the spherical Hankel function, we can prove the equivalence between Eq.(48) and (45).

**Case 3. Two spheres vibrating from uniform radial velocity**

After successfully solving one-sphere problems, we extend our approach to deal with the two-spheres radiation problem. As shown in Fig. 1, the two spheres vibrate with uniform radial velocity  $U_0$ . In the real calculation, we choose  $M$  to be ten. Sixty-six nodes are distributed on each sphere as shown in Fig.6. Figs. 7(a), 8(a) and 9(a) show the pressure contours of two dilating spherical sources at the horizontal plane of  $z=0$  for  $ka=1$ ,  $ka=2$  and  $ka=0.1$ , respectively, by using the SHIE [9]. Figs. 7(b), 8(b) and 9(b) are the corresponding results by using the present approach. After comparing our results with those of SHIE, good agreement is observed.

In the three cases, it is found that the analytical solution for the simple case (one sphere) can be derived by using our approach. For more than two spheres case, the boundary density is truncated to a finite number of terms. The collocation points are located on the real boundary to match boundary conditions and the unknown spherical harmonics coefficients can be easily determined. Since the error is attributed from the truncated finite number of terms of spherical harmonics coefficients, our approach can be seen as one kind of semi-analytical methods.

**4. CONCLUSIONS**

For the three-dimensional radiation problems, we have proposed a null-field integral equation formulation by using degenerate kernels and spherical harmonics in companion with adaptive observer systems. This method is a semi-analytical approach for Helmholtz problems with spherical boundaries since only truncation error in the spherical harmonics is involved. Although cases of one and two spheres are used, the present approach can

solve more general problems with multiple cylinders of arbitrary number, radii and positions without any difficulty. In addition, fictitious frequencies do not appear in the present formulation. A general-purpose program for solving radiation problem with arbitrary number, size and various locations of cylinders was developed. Pressure contours were compared well with the analytical and numerical solutions.

## 5. ACKNOWLEDGEMENT

This research was partially supported by the National Science Council in Taiwan through Grant NSC 96-2221-E-019-041.

## 6. REFERENCES

- [1] A.J. Burton and G.F. Miller, "The application of integral equation methods to numerical solution of some exterior boundary value problems," *Proc. Roy. Soc. Ser. A*, vol. 323, pp. 201-210, 1971.
- [2] H.A. Schenck, "Improved integral formulation for acoustic radiation problem," *J. Acous. Soc. Am.*, vol. 44, pp. 41-58, 1968.
- [3] J.T. Chen, K.H. Chen, I.L. Chen and L.W. Liu, "A new concept of modal participation factor for numerical instability in the dual BEM for exterior acoustics," *Mech. Res. Commun.*, vol. 26(2), pp. 161-174, 2003.
- [4] A.F. Seybert and T.K. Rengarajan, "The use of CHIEF to obtain unique solutions for acoustic radiation using boundary integral equations," *J. Acous. Soc. Am.*, vol. 81, pp. 1299-1306, 1968.
- [5] T.W. Wu and A.F. Seybert, "A weighted residual formulation for the CHIEF method in acoustics," *J. Acoust. Soc. Am.*, vol. 90(3), pp. 1608-1614, 1991.
- [6] L. Lee and T.W. Wu, "An enhanced CHIEF method for steady-state elastodynamics," *Engng. Anal. Bound. Elem.*, vol. 12, pp. 75-83, 1993.
- [7] S. Ohmatsu, "A new simple method to eliminate the irregular frequencies in the theory of water wave radiation problems," *Papers of Ship Research Institute* 70, 1983.
- [8] I.L. Chen, "Using the method of fundamental solutions in conjunction with the degenerate kernel in cylindrical acoustic problems," *J. Chin. Inst. Eng.*, vol. 29(3), pp. 445-457, 2006.
- [9] E. Dokumaci and A.S. Sarigül, "Analysis of the near field acoustic radiation characteristics of two radially vibrating spheres by the Helmholtz integral equation formulation and a critical study of the efficacy of the CHIEF over determination method in two-body problems," *J. Sound Vib.*, vol. 187(5), pp. 781-798, 1995.
- [10] J.T. Chen, W.C. Shen and P.Y. Chen, "Analysis of circular torsion bar with circular hole using null-field approach," *CMES*, vol. 12(2), pp. 109-119, 2006.
- [11] J.T. Chen and Y.T. Lee, "Interaction of water waves with an array of vertical cylinders using null-field integral equations," *The 14th National Computational Fluid Dynamics Conference*, Taiwan, 2007.
- [12] J.T. Chen, C.C. Hsiao and S.Y. Leu, "A new method for Stokes' flow with circular boundaries using degenerate kernel and Fourier series," *Int. J. Numer. Meth. Engng.*, vol. 74, pp. 1955-1987, 2008.
- [13] W.M. Lee and J.T. Chen, "Null-field integral equation approach for free vibration analysis of circular plates with multiple circular holes," *Comput. Mech.*, vol. 42, pp. 733-747, 2008.
- [14] J.T. Chen and A.C. Wu, "Null-field approach for piezoelectricity problems with arbitrary circular inclusions," *Engng. Anal. Bound. Elem.*, vol. 30, pp. 971-993, 2006.
- [15] A.F. Seybert, B. Soenarko, F.J. Rizzo and D.J. Shippy, "An advanced computational method for radiation and scattering of acoustic waves in three dimensions," *J. Acoust. Soc. Am.*, vol. 77(2), pp. 362-368, 1985.
- [16] M. Abramowitz and I.A. Stegun, *Handbook of mathematical functions with formulas, graphs, and mathematical tables*, Dover, New York, 1965.

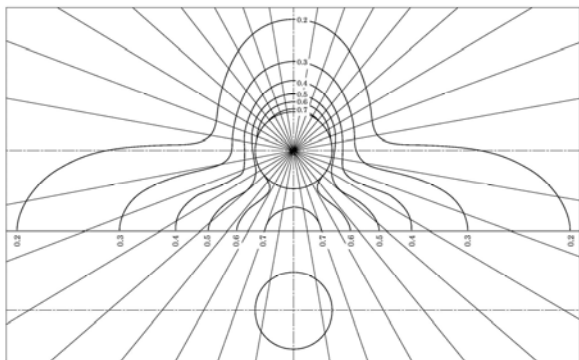


Fig. 7(a) Pressure contours by using the SHIE [9] ( $z=0$  and  $ka=1$ )

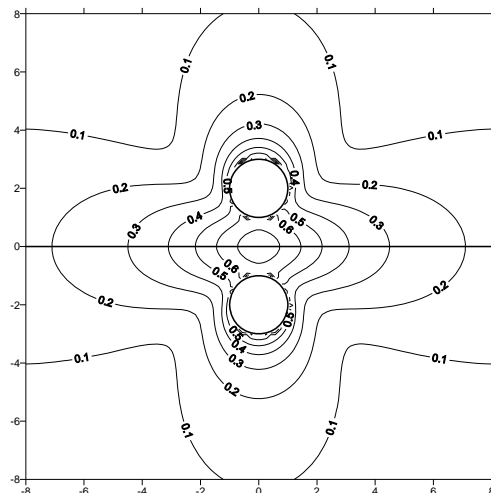


Fig. 7(b) Pressure contours by using the present approach ( $z=0$  and  $ka=1$ )

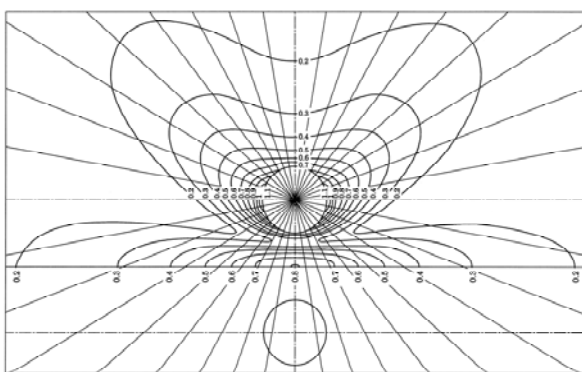


Fig. 8(a) Pressure contours by using the SHIE [9] ( $z=0$  and  $ka=2$ )

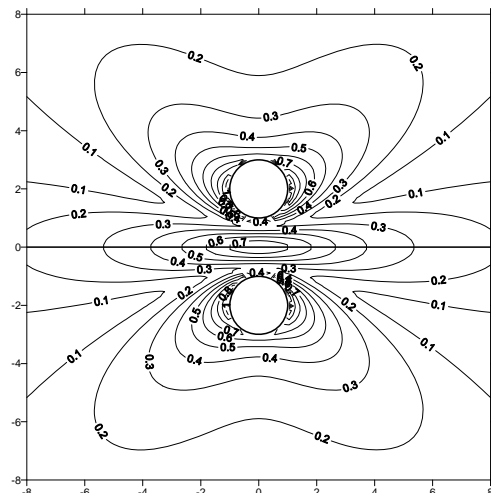


Fig. 8(b) Pressure contours by using the present approach ( $z=0$  and  $ka=2$ )

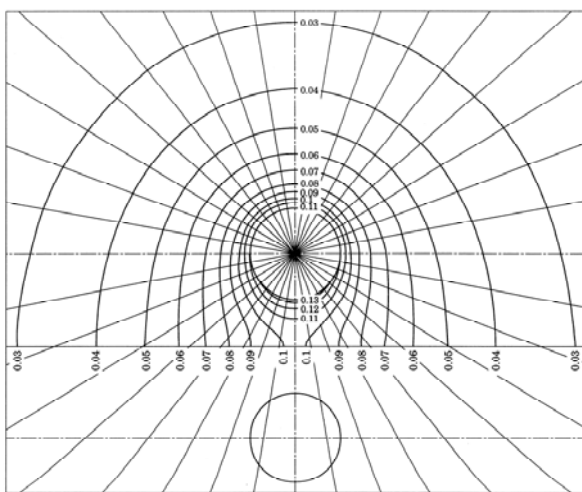


Fig. 9(a) Pressure contours by using the SHIE [9] ( $z=0$  and  $ka=0.1$ )

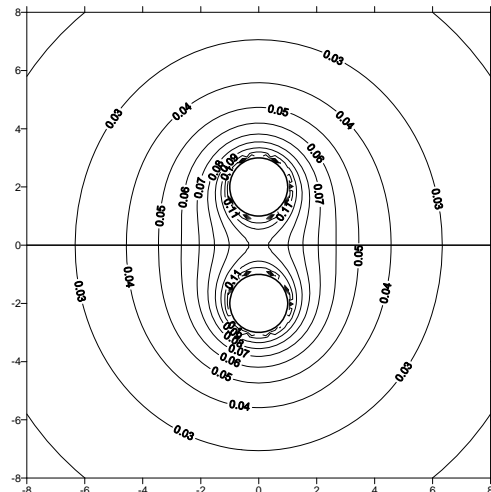


Fig. 9(b) Pressure contours by using the present approach ( $z=0$  and  $ka=0.1$ )